Liquid-Liquid Flows in an Inclined Pipe

Experimental measurements are reported of oil-water flows in a 20 cm ID pipe at mean velocities between 2.7 and 35 cm/s, at deviation angles θ from vertical between 0 and 65°, and at water flow rate fractions between 30 and 100%. The distribution of the water volume fraction α_w across a pipe section is obtained using local high-frequency probes. The mean water volume fraction in the section and the slip velocity V_s between oil and water are also determined. High V_s values (up to 50 cm/s) are measured at large deviation angles; they are associated with oil droplet swarms or continuous oil phase zones. Both α_w profiles and V_s values depend only on the mean water volume fraction and not on the total flow rate Q_t in the range investigated. At low oil volume fractions α_o, all droplets are concentrated close to the upper side of the pipe. At larger α_o values, a slower linear variation of α_w with the distance y from the axis is measured. A model is suggested relating the slope $\partial\alpha_w/\partial y$ in a vertical plane to the existence of internal density waves in the stratified mixture.

P. Vigneaux, P. Chenais
Physics Engineering Department
EPS Schlumberger
92142 Clamart, France

J. P. Hulin
Laboratoire d'Hydrodynamique et de
Mécanique Physique de l'ESPCI
75231 Paris Cedex 05, France

Introduction

Flowing mixtures of two immiscible liquids in pipes are frequently encountered in such domains as chemical and petroleum engineering. In the latter case, a significant amount of formation water is generally present inside oil-bearing reservoir rocks, particularly after an oil field has been under production for some time. Therefore, diphasic oil-water flows exist both inside the downhole producing wells and in the surface pipelines.

Both oil wells (particularly offshore) and pipelines have very variable deviation angles from vertical; some oil wells have even upward tilted zones. A key parameter influencing the structure of such inclined flows is the presence of gravity-driven buoyancy effects. The lighter phase (generally oil) gathers at the upper part of the flow tube section. In addition, the fluid velocity is nonuniform across the tube (water backflow often occurs at the bottom part). A knowledge of these phase stratification effects and of their dependence on the pipe deviation with respect to vertical, on the volume composition, and on the total flow rate is mandatory in order to understand the behavior of these flows and to develop suitable measurement procedures.

In spite of the practical interest of the problem, few data have been published on this topic to our knowledge. Most of the work on inclined diphasic flows has been performed on gas-liquid mixtures; semiempirical correlations between the pressure gradients along the flow and the flow rates of the various phases have been established (Beggs and Brill, 1972; Bonnecaze et al., 1971; Singh and Griffith, 1970). Maps relating the type of flow regime observed to the individual fluid flow rates have also been determined. More specific measurements have been performed on the velocity of large gas pockets in inclined pipes (Bendiksen, 1984; Maneri and Zuber, 1974; Mattar and Gregory, 1974; Zukoski, 1966). These measurements are applicable to analyze the slug flow regime where such large, fast-moving gas pockets separated by liquid slugs are observed. Models predicting the domains of existence for the various flow regimes have also been developed but are mostly adapted to near vertical or near horizontal flows (Dukler and Hubbard, 1975; Taitel and Dukler, 1976; Taitel et al., 1980).

However, the gas-liquid results cannot readily be translated into predictions for liquid-liquid flows. The surface tension and the density contrast are indeed much lower in the latter case. As will be shown, the dispersed phase takes the shape of small or very small droplets, not of large pockets. In addition, the relative velocities of the light and heavy phases are somewhat lower than in gas-liquid flows. In liquid-liquid flows, many publications analyze flows of heavy oil and water in horizontal pipes (Russel and Charles, 1959; Charles and Lilleleht, 1966) and seek to estimate the drag reduction due to the presence of a lubricating water film on the pipe walls. Zakin et al. (1979) have investigated the transport of oil as oil-in-water emulsions in pipes. Other published works deal with vertical oil-water flows (Barnea and Mizrahi, 1975; Foussat and Hulin, 1984; Nicolas and Witterholt, 1972). Measurements of the variation of the mean relative velocity V_s of the two phases give particularly interesting results. At global velocities low enough to avoid emulsifica-

tion, V_s depends only on the volume fraction for each phase and not on the total flow rate. This is a first indication that, due to the smaller contrast between the physical characteristics of the two phases, liquid-liquid flows may have a simpler behavior than gas-liquid flows.

We present here the results of systematic volume fraction profile measurements obtained using a high-frequency local volume fraction probe in water-kerosene flows (in this paper, kerosene will generally be refered to as "oil"). These measurements were performed in a 20 cm dia. pipe. A large range of total flow rates (2.7 to 40 m^3/h), deviation angles with respect to vertical (0 to 65°), and water flow rate fractions (30 to 95%) have been used.

In a first step, the analysis of water volume fraction α_w distribution maps, together with visual observations, gives qualitative information on the degree of stratification for the light phase and on the various possible flow regimes. From these maps, the average fraction α_{wm} in the cross section is obtained as well as the average slip velocity V_s between the two phases. We shall seek to verify whether, as in vertical flows, V_s depends only on α_{wm} and not on the global flow rate Q_t, provided the pipe diameter is large enough.

Finally, a detailed study of the oil volume fraction variation in a vertical plane will determine the physical parameters controlling those profiles.

Experimental Set-up and Measurement Procedure

The diphasic flow is generated by injecting oil and water through separate pipes at the bottom of a 14 m long flow channel (20 cm ID) that can be tilted at any angle between horizontal and vertical. The measurement section is located 2 m below the top in order to allow for a sufficient stabilization length. Deviation angles θ of 0, 5, 15, 25, 45, and 65° from vertical were used.

After leaving the pipe, the mixture goes through a gravity separator before oil and water are recirculated through separate pumping and metering circuits. Measurements are performed at Q_t values of 40, 27, 13.5, 6.7, and 2.7 m^3/h. A maximum total flow rate Q_t of 40 m^3/h (corresponding to a mean velocity of 35 cm/s) is used in order to avoid emulsification occurring due to poor oil-water separation at higher values.

For all θ and Q_t values, the distribution of the local volume water fraction α_w is determined for five different water flow rate fractions x_w (95, 90, 70, 50, and 30%). In some isolated cases, data points corresponding to x_w = 10% have also been taken. Turbine flowmeters are used to measure the individual flow rates with a precision better than 1%.

We did not use mixtures with a high oil volume fraction α_o because of flow stabilization problems; at low velocities and large α_o values, the water remaining at the walls does not move easily and is only carried away very slowly by the main oil flow.

We use a small high-frequency (1 GHz) impedance probe with a 0.5 mm dia. tip which is similar to those described by Kobori and Terada (1978) and Reimann et al. (1977). The measurement is based on the difference between the probe impedance value when the probe tip is immersed in oil or water. Due to the high frequency used, the probe is mostly sensitive to dielectric constant variations. A HF-bridge continuous-wave detection circuit transforms these impedance variations into a DC signal that is then fed into a thresholding system. A logic-type output is finally obtained with one level corresponding to oil and the other to water (Vince and Lahey, 1980).

The local time-averaged volume fractions for a given phase are equal to the percentage of time during which the output has the corresponding value. We performed calibration measurements in large vertical flows where the relation between the volume fraction and the flow rate fraction can be approximated easily; from these results we estimate the precision on the absolute value for the local water volume fraction α_w to be ±2% in the whole range (and down to ±0.5% close to α_w = 0 and 100%). Impedance probes are well adapted to oil-water flow measurements because of the large dielectric constant contrast between the two liquids. Optical fiber probes, which are often used in gas-liquid flows, are mainly sensitive to optical index variations, with a poor contrast between oil and water (Jones and Delhaye, 1976).

In our experiments the impedance probe is mounted inside a 30 cm long rotating section of the flow tube, Figure 1; it can, in addition, translate all along a diameter of the tube. The rotation amplitude is 90°; in this way, half of the total section area is explored. We verified that no flow asymmetry due to the injection system occurs by checking in vertical flows the circular symmetry of the volume fraction distribution; therefore we assume simply that the volume fraction profile is symmetrical with respect to a vertical plane in order to draw the volume fraction distribution in the whole pipe section.

After a flow stabilization time (5 min to 1 h) sufficient to obtain stable α_w readings, the impedance probe is scanned downward across the flow section. The stabilization time is higher at low flow rates, low deviations, and high oil volume fractions.

The probe scanning is fully computer controlled; the local value of α_w is measured at points spaced 5 or 10 mm along a pipe diameter (closely spaced points are needed when concentration gradients are high). For a given angular position of the flow section, the probe is moved from the upper side of the section (where the density of oil droplets is usually higher) toward the lower side. When the scanning across a diameter is completed (or when no oil droplets are detected), then the measurement section is rotated by 10 or 20° and another set of data is taken along the diameter in this new position. Acquiring each data point takes about 1.5 min; a complete volume fraction map is obtained in 1 to 2 h. After the acquisition, lines of constant volume fraction in the flow section are obtained from the experimental results through a smoothing and interpolation procedure, Figures 2, 4, and 5. In order to draw these maps, we assume that the water volume fraction distribution is symmetrical with respect to the pipe diameter located in a vertical plane.

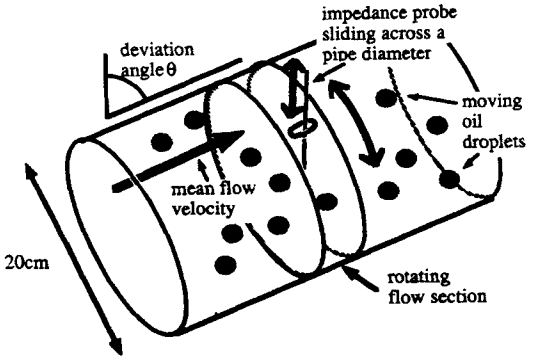

Figure 1. Experimental measurement set-up.

Qualitative Analysis of Fluid Distribution and Visual Observations

Figure 2a shows a map obtained with a vertical flow tube ($\theta = 0°$) for a water flow rate fraction $x_w = 70\%$ and a total flow rate $Q_t = 40$ m^3/h (the corresponding mean superficial velocity $V_t = Q_t/S$ is $\simeq 35$ cm/s [S is the pipe section]). The distribution of α_w has a nearly cylindrical symmetry and, in the central part of the pipe, α_w varies by less than 2% (solid lines correspond to α_w values multiple by 10%, broken lines correspond to values separated by 2%). The profiles of Figure 2b have been obtained for the same Q_t and α_w values as in Figure 2a but with a deviation angle $\theta = 5°$ with respect to vertical. We observe that even such a small deviation of the flow tube induces significant gradients of α_w (the upper side of the pipe is oriented upward on the maps).

Visually, in vertical flows, for $\alpha_{wm} > 30\%$, a steady motion of oil droplets with a constant velocity is observed, Figure 3a. For $\alpha_{wm} < 20$–30%, the water phase becomes dispersed and a continuous oil phase carrying water droplets is observed in the center part of the pipe. Close to the transition, the flow becomes intermittent and continuous oil and water phases are alternately observed.

On the other hand, in deviated flows, even at moderate inclination angles, the flow becomes intermittent when the fraction $\alpha_{om} = 1 - \alpha_{wm}$ of oil increases to about 10%. Droplet swarms with an high oil volume fraction appear and push in front of them water that flows back below the swarms in the reverse direction, Figure 3b. The local volume fraction of oil decreases on the lower side of the pipe section and large recirculation cells are observed when $\alpha_{om} > 25\%$. Let us emphasize that the droplets do not coalesce into large pockets of oil; this result is very different from gas-water flows where large gas pockets are very often observed in the slug and churn flow regimes.

At large deviations such as $\theta \geq 45°$ and low α_{wm} values, nearly all the oil droplets are often localized in the upper part of the pipe. This is observed for instance in Figure 4a for $\theta = 45°$, $Q_t = 27$ m^3/h ($V_t = 23$ cm/s), and for a water flow rate fraction $x_w = 90\%$ (in Figures 4 and 5, only constant α_w lines corresponding to α_w values multiple of 10% are shown). In this case, too, the flow is intermittent and fast-moving droplet swarms are observed; very little oil is present in the rest of the flow and water backflow also occurs below the swarms, Figure 3c. At $\theta = 65°$, the concentration in the upper part would get still higher and a nearly continuous, fast-moving channel of oil carrying water droplets may appear. When x_w decreases to 30% at the same deviation angle $\theta = 45\%$ and total flow rate $Q_t = 27$ m^3/h, Figure 4b, the oil droplet distribution gets less segregated although the spatial gradients of α_w remain large.

Hence, while the segregation of the oil phase is almost complete at low mean oil volume fractions α_{om}, more oil is brought into the lower part of the pipe section inside recirculation cells at higher α_{om} values. This can be done either by decreasing x_w at constant Q_t, Figure 4, or by increasing Q_t at constant θ and x_w values. This latter effect is shown in the maps of Figure 5, which correspond to $\theta = 65°$ and $x_w = 50\%$. Although this x_w value is rather large, almost all oil is localized on the upper side of the pipe section, Figure 5a, at the lower flow rate $Q_t = 6.7$ m^3/h ($V_t = 5.9$ cm/s); at the higher flow rate $Q_t = 40$ m^3/h ($V_t = 35$ cm/s) many more oil droplets are detected in the lower part of the flow tube section, Figure 5b.

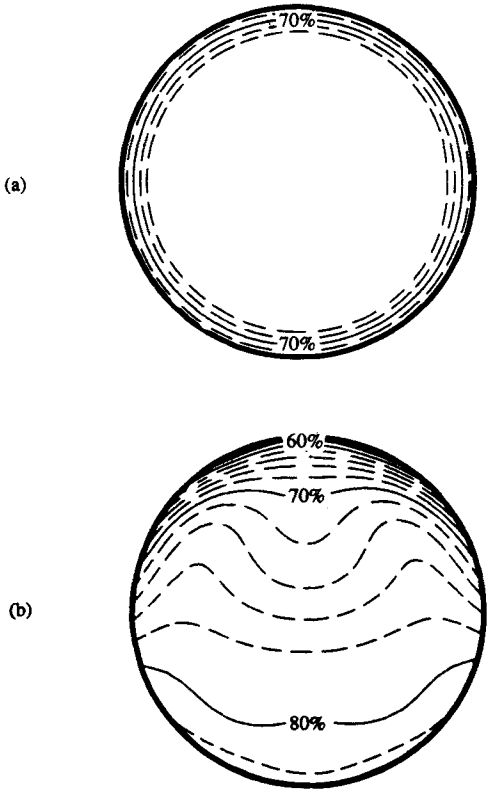

Figure 2. Constant volume fraction α_w lines for a vertical and a deviated pipe at the same total flow rate Q_t and water flow rate fraction x_w.

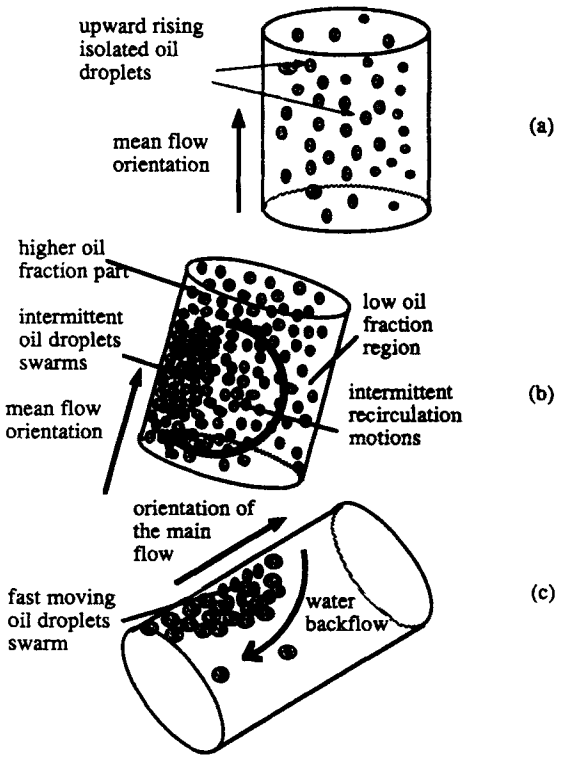

Figure 3. Several flow regimes observed in vertical and deviated oil-water flows.

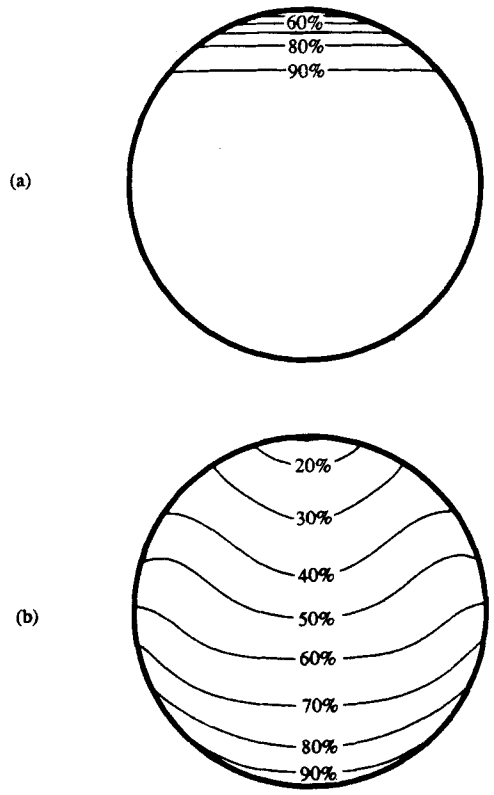

Figure 4. Constant local α_w lines for two water flow rate fractions at the same total flow rate and deviation angle values.

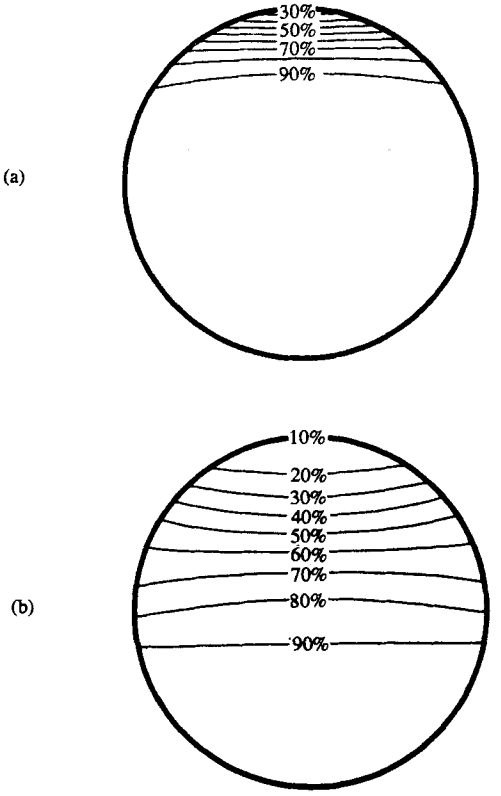

Figure 5. Constant local water volume fraction lines for two total flow rates at the same deviation angle and water flow rate fraction values.

During all our experimental runs the size of individual droplets did not vary significantly and was of the order of 2–6 mm. It is however likely that at larger mean flow velocities the higher turbulence level would emulsify the mixture, resulting in a smaller size of the droplets and reduced stratification effects.

Relation between Volume and Flow Rate Fractions of the Flowing Mixture and the Mean Slip Velocity between Oil and Water

The mean water volume fraction α_{wm} is obtained from an average on the total flow section of the α_w values in the maps described above. Figure 6 shows the variation of α_{wm} with the water flow rate fraction $x_w(x_w = 1 - x_o)$ at two different flow rates, Q_t = 6.7 m^3/h (open squares) and 40 m^3/h (black diamonds), and the three deviation angles listed on the curves. While at low deviations and large velocities α_{wm} and x_w differ by less than 5% in the range investigated ($0.3 < x_w < 1$), the difference increases when the flow tube is more inclined. At Q_t = 6.7 m^3/h and $\theta = 65°$, α_{wm} remains above 90% even for x_w = 30%.

In order to make a quantitative analysis of the difference between x_w and α_{wm}, let us show now that the curves of Figure 6 can be used to estimate the relative slip velocity V_s of the oil and water phase. Let us first define mean oil and water velocities V_o and V_w by:

$$V_o = \frac{Q_o}{\alpha_{om} S} = \frac{Q_t}{S}\frac{x_o}{\alpha_{om}} \tag{1}$$

$$V_w = \frac{Q_w}{\alpha_{wm} S} = \frac{Q_t}{S}\frac{x_w}{\alpha_{wm}} \tag{2}$$

where Q_o and Q_w are the oil and water volume flow rates and S is the pipe cross section. Equations 1 and 2 give exactly the mean water or oil velocity only if the velocity or volume fraction profiles are uniform. Then, we define the average slip velocity as the difference between these mean velocity values, $V_s = V_o - V_w$. Since $x_o = 1 - x_w$, $\alpha_{om} = 1 - \alpha_{wm}$, and $x_o = 1 - x_w$, one

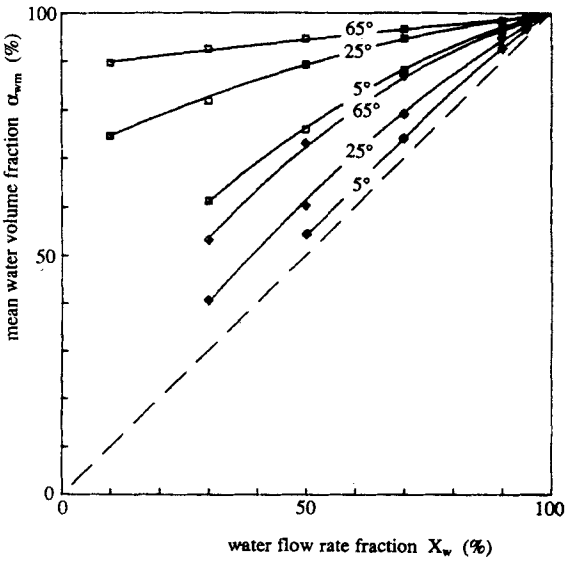

Figure 6. Mean water volume fraction variation at two flow rate values and three deviation angles.

obtains:

$$V_s = \frac{Q_t}{S} \frac{\alpha_{wm} - x_w}{\alpha_{wm}(1 - \alpha_{wm})} \tag{3}$$

Let us note that near $\alpha_{wm} = 0$ or 1, the computation of V_s from Eq. 3 becomes indeterminant and the uncertainty on its value is high.

In a mixture flowing with uniform velocity and volume fraction profiles, V_s gives directly the velocity difference between the two fluids. However, in stratified flows, the fluid distribution and velocities are very heterogeneous (because of stratification and recirculation effects); V_s is then only an order of magnitude estimate of the relative velocity of oil and water in regions of high oil concentration. We shall see, however, that V_s gives very useful indications on the presence of fast-moving oil droplet structures such as swarms or continuous oil channels.

Figure 7 shows the variation of V_s with the mean water volume fraction α_{wm} at three different deviation angles $\theta = 5$, 25, and 65°. The data points correspond to the whole range of x_t and Q_t values used in our experiments. The most striking feature is that, at a given deviation angle and within the experimental uncertainty, V_s depends only on the volume fraction α_{wm} and not on the total flow rate Q_t. In contrast, when one replaces α_{wm} by x_w as the horizontal coordinate, the variation of V_s with x_w does depend on Q_t. This confirms and generalizes similar results reported by Nicolas and Witterholt (1972) for vertical flow using vertical pressure gradient measurements.

Let us emphasize that $V_s(\alpha_{wm})$ may start to vary with Q_t at very high flow velocities that could not be obtained in our experiments. Emulsification should then take place due to the higher degree of turbulence and both the droplet size and the velocity difference between oil and water will vary. An important goal of future experiments will be to determine the Q_t threshold value above which V_s starts to decrease at a fixed α_{wm} value.

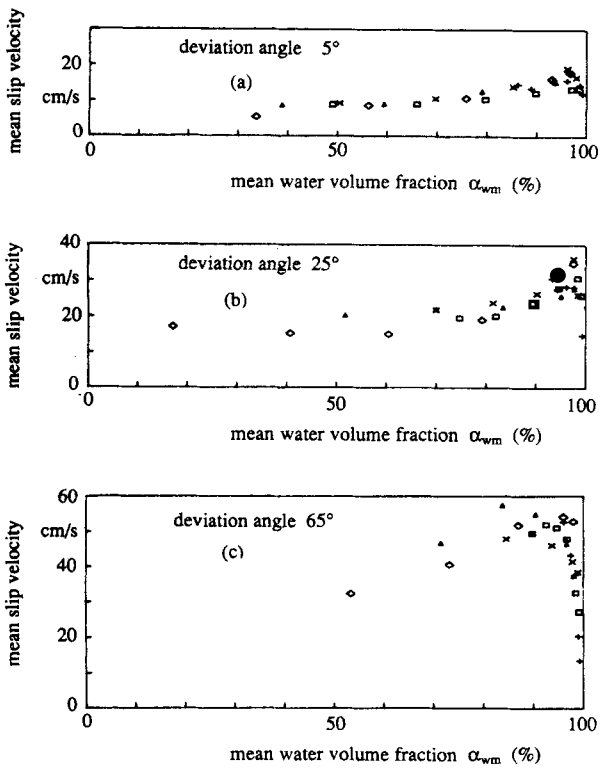

Figure 7. Mean slip velocity variation with mean water volume fraction at three deviation angles.

In addition, V_s will probably not remain independent of Q_t for pipe diameters D smaller than the value $D = 20$ cm used in the present experiments both because of the increase of the velocity at a given Q_t value and because of the higher relative influence of the wall effects.

The slip velocity V_s increases with the deviation θ. This is rather unexpected at a first glance: increasing θ reduces indeed the gravity component parallel to the pipe axis and would therefore seem to reduce the rise velocity. From our measurements, three domains of deviation angles can grossly be separated: low, medium, and high.

At low deviation angles ($\theta = 0$–5°), the velocity V_s decreases with α_{wm}, Figure 7a, from 15–20 cm/s (low concentrations of droplets with little interaction) down to 10 cm/s (strongly interacting droplets). At low oil concentrations, V_s is comparable to the rise velocities V_r of single oil droplets in water (around 15 cm/s) as determined by Nicolas and Witterholt (1972).

At medium deviation angles, ($\theta = 15$ to 45°), V_s has a maximum value $V_s \simeq 30$ cm/s (much higher than the relative velocity V_r of isolated droplets) around $\alpha_{wm} = 0.95$, Figure 7b. We suggest that this high value is associated with fast-moving droplet swarms where almost all the oil is concentrated, Figure 3c. At lower oil concentrations, V_s decreases toward V_r. At higher oil volume fractions, slower moving recirculating cells are observed instead of independent swarms; the oil fraction in the lower part of the pipe section increases and backflowing droplets reduce the mean oil velocity. The relative velocity between oil and water is also reduced by the higher interaction between droplets. The range of α_{wm} values where swarms are observed broadens at higher deviation angles because of the stronger stratification effect.

We believe, that, as a first approximation, the fast-moving droplet swarms are the equivalent in liquid-liquid flows of large Taylor-type gas bubbles observed in gas-liquid flows. Taylor bubbles have a width of the order of the pipe section and are observed particularly in well-established slug flow regimes (Taitel et al., 1980) when the volume fraction of gas gets above about 10%. Their rise velocity V_T is mostly determined by a balance between gravity and inertia; V_T is almost independent of the bubble length and has a maximum around a deviation angle $\theta \simeq 45°$ (Bendiksen, 1984; Maneri and Zuber, 1974; Zukoski, 1966) with:

$$V_T(45°) = 0.6\sqrt{gD} \tag{4}$$

where g is the gravitational acceleration and D the flow tube diameter.

In the oil-water flows we have investigated, large continuous oil pockets similar to Taylor bubbles cannot be observed: the oil-water interface is not stable enough and the pockets would get broken up very quickly into small droplets. However, swarms of closely packed oil droplets surrounded by oil-free water may have a similar behavior: the water velocity through these may be rather low and they will move as independent entities.

Let us estimate the velocity of these swarms. Introducing into Eq. 4 an additional factor taking into account the density contrast between oil and water that is much lower than between

water and air, we obtain:

$$V_{swarm} \simeq 0.6 \sqrt{\frac{\rho_{water} - \rho_{oil}}{\rho_{water}}} \sqrt{gD} \qquad (5)$$

Using our experimental parameters, Eq. 5 gives $V_{swarm} \simeq 42$ cm/s. This is the right order of magnitude and the difference with the (lower) experimental value is not surprising due to the noncontinuous structure of the swarms. An additional factor taking into account the nonzero percentage of water inside them should indeed be included in Eq. 5.

In conclusion, at medium deviations and high water concentrations, the intermittent flow of oil in a continuous water phase is associated with well-defined swarms moving inside water, with very few isolated droplets. At lower α_{wm} values, all of the pipe cross section gets invaded and recirculation cells moving with the main flow are observed.

At high deviation angles ($\theta = 65°$), still larger V_s values are measured, Figure 7c; for instance, one has $V_s > 50$ cm/s at $\alpha_{wm} \simeq 90\%$. We suggest that the oil concentration in the upper part of the pipe section is high enough to create a zone where the oil phase is continuous. In such zones, the oil flow is less slowed down by the water than in the swarm configuration and V_s can then get even larger than the value given by Eq. 5. V_s decreases at low α_{om} values because there are not enough oil droplets for the continuous oil zone to build up. At high oil concentrations V_s also decreases because recirculation cells appear; then, oil droplets moving backward in the lower part of these cells reduce the mean oil velocity.

Analysis of the Water Local Volume Fraction Profile across a Pipe Diameter in Vertical and Deviated Flows

For vertical flows, the variation of α_w in the flow section should have a nearly circular symmetry. This is verified in Figure 8, which shows for $\theta = 0°$ and $Q_t = 27$ m^3/h ($V_t \simeq 23.5$ cm/s) the variation of α_w with the distance y to the pipe axis across a diameter. Five different mean water volume fractions $\alpha_{wm} = 97$, 93, 76, 57, and 40% have been used. At low oil volume fractions, the α_w profile is very curved, with a minimum on the pipe axis and values much closer to 100% near the pipe walls. Below $\alpha_{wm} \simeq 85\%$, the profile becomes flat: α_w varies by less than 5% in relative value up to about 2 cm from the pipe wall.

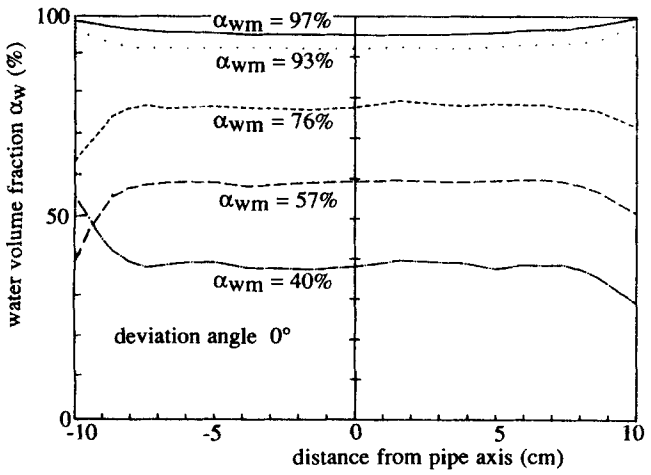

Figure 8. Variation of α_w across a vertical pipe diameter for a constant total flow rate and five mean water volume fraction values.

These data correlate very well with previously reported α_w measurements obtained in a smaller (6 in [15.25 cm] ID) pipe (Foussat and Hulin, 1984). In this previous work, we performed simultaneously local velocity measurements using an acoustic Doppler flowmeter; the transition toward a flat α_w profile coincides with the appearance of flat velocity profiles and lower velocity values.

We conclude that at high oil fractions ($\alpha_o > 15\%$), oil droplets have large interactions between themselves so that the influence of the wall becomes negligible above a distance $\simeq 2$ cm. Outside of this wall layer, the whole oil mixture has a pistonlike flow, with the relative velocity of oil and water determined only by the mean α_{wm} value. At low oil volume fractions, the interaction with the wall plays a more important part: larger velocity and α_w gradients are present in the whole pipe section.

In deviated flows, even at low θ values, large gradients of α_w are observed in the central part of the flow tube. For instance, Figure 9 shows three typical diametral profiles obtained at the same θ (15°) and Q_t (40 m^3/h; $V_t \simeq 35$ cm/s) values for different mean water volume fractions $\alpha_{wm} = 97$, 60, and 8.5% (the latter figure corresponds to $x_w = 10\%$ and may be biased by water accumulation at the pipe walls and long stabilization times for high oil content flows). The profiles correspond to the pipe diameter located in the vertical plane containing the pipe axis.

- For $\alpha_{wm} = 97\%$, all the oil droplets are segregated in the upper part of the measurement diameter and the local volume fraction α_w increases steeply to more than 95% within a few cm from the upper wall (type 1 profile).
- For $\alpha_{wm} = 60\%$, the amount of oil is sufficient to invade the whole pipe, α_w has a smooth linear variation along most of the diameter; the influence of the wall becomes apparent in a curvature of the profile only within 2 cm of the upper and lower walls (type 2 profile).
- For $\alpha_{wm} = 8.5\%$, most of the water is located in the bottom part of the pipe section although the decrease of α_w with the dis-

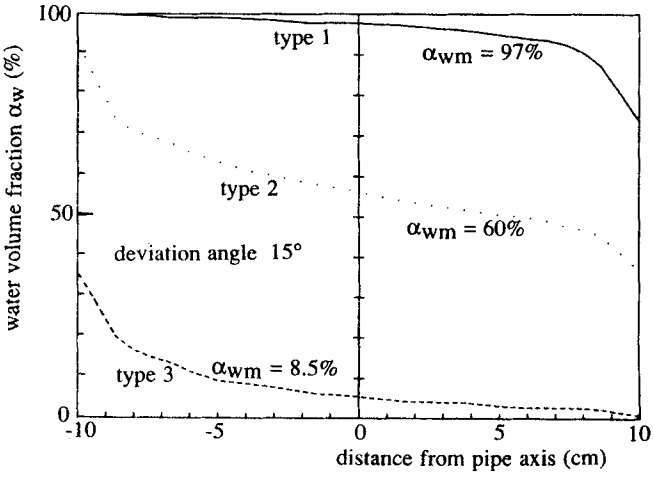

Figure 9. Variation of α_w across a pipe diameter at a constant total flow rate Q_t for three water flow rate fractions.

Deviation angle $\theta = 15°$
$x_w = 95$, 50, and 10%

tance from the lower end of the measurement diameter is smoother than in case 1 (type 3 profile).

It is clear that the distance to the pipe wall is an important parameter for profiles of type 1 and 3 (as for the vertical α_w and velocity profiles obtained in vertical flows at low oil volume fractions). Type 2 profiles are analogous to the piston-type flows observed for vertical flows in the intermediate α_{wm} value range but gravity-induced stratification effects are an important additional factor.

Influence of Mean Water Volume Fraction and Total Flow Rate on the Flow Structure at Medium Water Contents

Figure 10 shows three type 2 diametral profiles obtained at the same 15° pipe deviation as in Figure 9. The two lower profiles correspond to very different total flow rates Q_t = 40 m³/h (dotted line) and 6.7 m³/h (solid line) but to the same mean water volume fraction $\alpha_{wm} \simeq 60\%$; the corresponding V_t values are 35 and 5.9 cm/s. In spite of the large flow rate difference, the two profiles coincide within the experimental uncertainty; this result is valid for all profiles that we have determined. We conclude that the water distribution is solely determined by the mean volume fraction value α_{wm}; in the range of values we have used, the total flow rate Q_t does not influence the profile of α_w. This result is also approximately valid for profiles of types 1 and 3 as well as for the distribution outside the vertical plane.

The third curve (broken line) in Figure 10 corresponds to a higher mean water fraction $\alpha_{wm} \simeq 77\%$ and to a flow rate of 40 m³/h ($V_t \simeq 35$ cm/s). This profile is shifted upward with respect to the other two but the slope $\partial\alpha_w/\partial y$ in the center part of the measurement section remains the same.

In order to analyze these results more quantitatively, we determined the slope $\partial\alpha_w/\partial y$ by a linear regression on data points close to the pipe axis on the measurement diameter. Figure 11 shows the variation of $\partial\alpha_w/\partial y$ (expressed in percent of water volume fraction per cm) with α_{wm} at two different deviation angles θ = 25° and θ = 65°.

For θ = 25° (data points marked + in Figure 11), $\partial\alpha_w/\partial y$ is constant and independent of α_{wm} for $\alpha_{wm} < 80\%$. The variation is

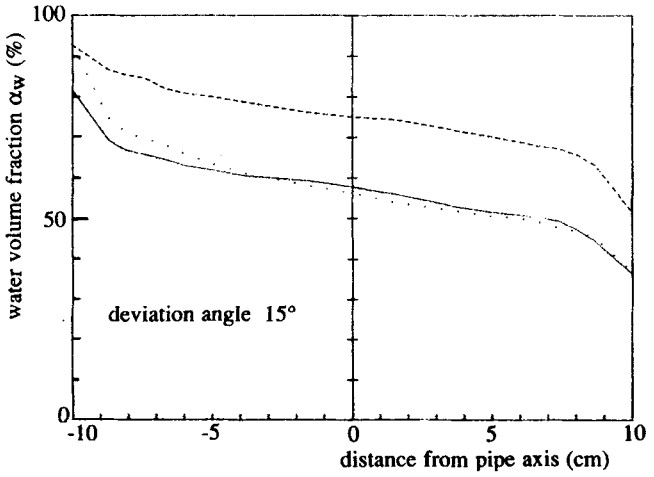

Figure 10. Water volume fraction profiles across a pipe diameter for two total flow-rate and water flow rate fraction values.
Deviation angle θ = 15°

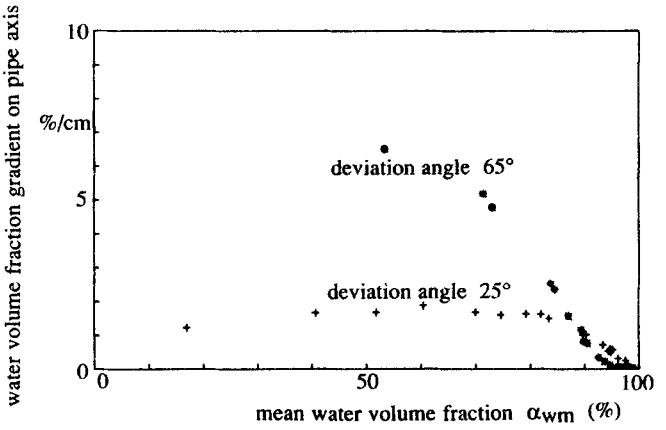

Figure 11. Local water volume fraction gradient $\partial\alpha_w/\partial y$ variation with mean water fraction α_{wm} for two deviation angles.

similar for θ = 5° and θ = 15° (obviously $\partial\alpha_w/\partial y = 0$ for $\theta = 0$). As expected, the region where $\partial\alpha_w/\partial y$ is constant coincides with the domain of existence of type 2 curves such as shown in Figures 9 and 10. Therefore, at a given θ value, $\partial\alpha_w/\partial y$ is the same in the central part of the pipe for all type 2 curves (independent of x_t and Q_t); α_w profiles corresponding to different mean α_{wm} values are shifted parallel to the α_w axis but retain the same shape. In addition, at a given location the local α_w always increases with the mean value: no intersection between profiles occurs.

For θ = 65° (data points marked * in Figure 11), $\partial\alpha_w/\partial y$ steadily increases when α_{wm} decreases but, as for the other curve, does not depend on Q_t. The stratification effects become too important for type 2 curves to be observed, at least in the x_w range that we have used. For θ = 45°, $\partial\alpha_w/\partial y$ seems to level off at $\alpha_{wm} \simeq 70\%$ (these data points are not shown).

Relation between Water Fraction Gradient, Deviation Angle, and Mean Slip Velocity

Let us first analyze type 2 profiles observed at intermediate water fractions. The parameter $\partial\alpha_w/\partial y$ just introduced above is clearly crucial to characterize the phase stratification.

Due to the continuous variation of α_w in the whole pipe section, internal gravity-driven waves may appear and induce oscillations of α_w. Such waves are commonplace in stratified media (Lighthill, 1978) and we believe that the recirculation cells observed at intermediate water volume fractions may be associated with them. If this hypothesis is right, then the mean slip velocity V_s between oil and water should be closely related to the velocity V_i of these internal waves.

Without attempting to solve completely the wave equation in the confined pipe geometry, let us evaluate an order of magnitude of V_i by:

$$V_i \approx \frac{N\lambda}{2\pi} \tag{6}$$

λ is the wavelength of the waves and is of the order of $2D$ (D = pipe diameter), N is the Brunt-Väisälä angular characteristic frequency corresponding to stationary gravity-induced density

oscillations in a stratified medium with:

$$N = \sqrt{\frac{-g \sin\theta}{\rho_m}\frac{\partial \rho_m}{\partial r}} = \sqrt{-2g \sin\theta \frac{\rho_w - \rho_o}{\rho_w + \rho_o}\frac{\partial \alpha_w}{\partial r}} \qquad (7)$$

(we used $g \sin\theta$ instead of g since we are interested in the radial density gradients in a vertical plane; ρ_m is the mean local density of the mixture).

We have plotted in Figure 12 (black squares) the variations of V_s given by Eq. 3 against the corresponding values of the internal wave velocity V_i estimated from Eqs. 6 and 7; only deviation angles of 45° and below and α_w values giving type 2 profiles have been used, and the corresponding data points have been averaged. The variation is linear within the experimental uncertainty on the values of V_s and $\partial\alpha_w/\partial y$.

In order to separate the influence of the internal density waves and of the drift of the individual droplets, we have also plotted in Figure 12 (open squares) a corrected slip velocity $V_{sc}(\theta)$ computed by subtracting from $V_s(\theta)$ a drift velocity $V_d(\theta)$. $V_d(\theta)$ is estimated by assuming that the flow is nonintermittent, with a velocity uniform across the pipe section as is the case for $\theta = 0$ (in this latter case, internal waves do not appear because, from Eqs. 6 and 7, their velocity goes to 0). Such a drift flow should be driven by the component $g_f = g \cos\theta$ of gravity parallel to the pipe axis; since the vertical rise velocity V_d of bubbles or droplets with that size varies as $\sqrt{g}$, one can take $V_d(\theta) = V_s(0)\sqrt{\cos\theta}$. We obtain therefore the following estimation of the component $V_{sc}(\theta)$ in the slip velocity purely associated with internal density waves:

$$V_{sc}(\theta) = V_s(\theta) - V_s(0)\sqrt{\cos\theta} \qquad (8)$$

[as required by Eqs. 6 and 7 we verify that $V_{sc}(\theta)$ goes to 0 for $\theta = 0$].

We see from Figure 12 that $V_{sc}(\theta)$ is proportional (and very close) to V_i on the whole deviation range, although this quantitative agreement is probably fortuitous due to the neglect of many numerical factors. The curves of Figure 12 however demonstrate that the variation of V_s with θ is closely associated with internal waves induced by the stratification that shows up visually as recirculation cells moving with the flow.

The shape of type 1 and type 3 curves is more difficult to predict since the presence of the wall and the velocity gradients near it have to be taken into account. In case 1, the decrease of α_w with the distance from the wall is approximately exponential but the number of points is not large enough for more quantitative interpretations.

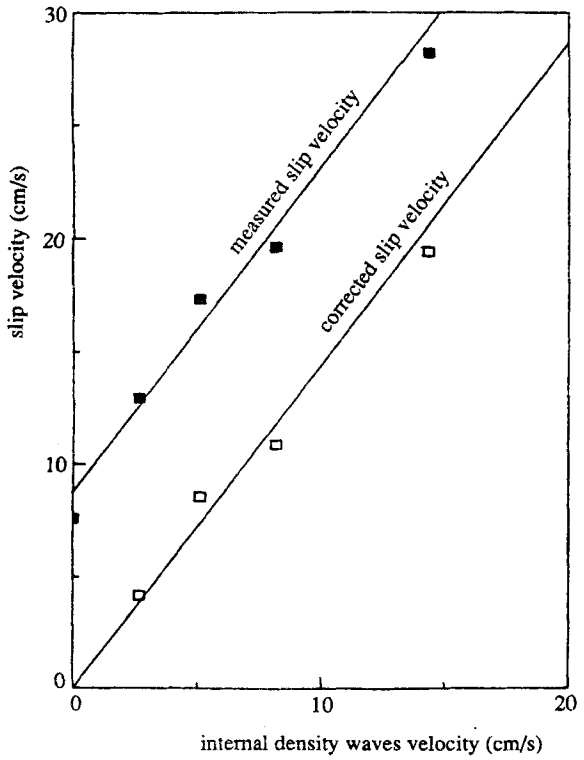

Figure 12. Variation of mean slip velocity V_s between oil and water (measured and corrected from individual droplets drift) with estimated velocity V_i for density-gradient-induced internal waves.

Conclusions

The experimental results related above show that even at moderate tilt angles, the oil distribution in the flow section and the mean relative (slip) velocity between the light and the heavy phase are strongly influenced by the pipe deviation:

- The oil fraction profiles and the slip velocity depend only on the mean volume composition of the mixture and on θ not on the total flow rate Q_t (in the range investigated).
- At low oil mean volume fractions α_{om} $(=1 - \alpha_{wm})$, all the oil droplets are concentrated within a few cm of the upper side of the flow pipe.
- At $\theta > 10°$ and low α_{om} values (typically between 5 and 20%), fast-moving droplet swarms are observed; they seem equivalent to the gas pockets present in gas-liquid slug flows. The oil droplets do not coalesce inside the swarms because of the greater instability of the water-oil interface. Outside the swarms, the oil concentration remains very small.
- At large deviation angles ($\theta > 60°$) and α_{om} values around 10%, very large oil-water relative velocities V_s are measured (>65 cm/s); regions where the oil phase is continuous appear in the upper part of the pipe section.
- At high enough α_{om} values (typically >20%) for $\theta \leq 45°$, large recirculating motions of oil droplets are observed in the central part of the flow. In this zone α_o varies linearly along a diameter in a vertical plane with a slope $\partial\alpha_w/\partial y$ depending almost only on the deviation angle θ. This phenomenon seems to be closely associated to internal gravity-induced waves of the type commonly observed in stratified media.

A surprisingly clear-cut result of these experiments is the weak influence of the global flow rate Q_t on the volume fraction α_w profiles and on the mean relative oil-water velocity. This shows that both short-range interactions between droplets (due for instance to the turbulence they induce) and density gradient effects are larger than the influence of the turbulence due to the mean flow. Measurements at higher velocities will be necessary to determine the threshold Q_t value above which emulsification effects modifying α_{wm} and V_s become important.

At high oil volume fractions, the structure of the mixture as well as the possible transition toward a continuous oil phase are problems that are closely related to the physics of foams. It is clear that the physical properties of the oil used plays a domi-

nant role; oils with a varying viscosity, surface tension, or density will give oil-water interfaces of different stabilities and the flow structure may be deeply modified. Other parameters such as the water salinity may also influence the droplet break-up and coalescence process. More experiments are needed to determine whether and when continuous pockets of oil can exist and, on the contrary, when an emulsification of the mixture into a suspension of microscopic droplets occurs.

Acknowledgment

We wish to thank A. E. Dukler, E. Guyon and T. J. Plona for their many comments and suggestions, and R. Coudol for his invaluable technical assistance.

Notation

D = flow tube internal diameter
g = gravity acceleration
g = gravity acceleration component along the flow ($=g \cos \theta$)
N = frequency of gravity-induced density oscillations in a stratified medium
Q_o = oil volume flow rate
Q_t = total volume flow rate (oil + water)
Q_w = water volume flow rate
S = flow tube cross section
V_d = drift velocity of individual droplets excluding effect of collective motions
V_i = velocity of internal gravity waves in a stratified medium
V_r = rise velocity for a single oil droplet in a stationary fluid
V_s = relative slip velocity between oil and water
V_{sc} = corrected slip velocity value, $=V_s - V_d$
V_{swarm} = velocity of oil droplet swarms
V_t = mean superficial fluid velocity, $=Q_t/S$
V_T = velocity of Taylor-type large gas bubbles
x_o = oil flow rate fraction relative to total flow rate, $=Q_o/Q_t$
x_w = water flow rate fraction, $=Q_w/Q_t = 1 - x_o$ in the present experiments
y = distance from pipe pipe axis, measured along the flow tube diameter located in a vertical plane

Greek letters

α_o = time-averaged local oil volume fraction
α_{om} = average of α_o over the flow tube cross section
α_w = time averaged local water volume fraction, $=1 - \alpha_o$ in the present experiments
α_{wm} = α_w average over the flow cross section, $=1 - \alpha_{om}$ in the present experiments
λ = wavelength of gravity waves in a stratified fluid
ρ_o = oil density
ρ_w = water density
ρ_m = local mean density of oil-water mixture
θ = pipe deviation angle with respect to vertical, $=0$ for a vertical flow tube

Literature Cited

Barnea, E., and J. Mizrahi, "Separation Mechanism of Liquid-Liquid Dispersions in a Deep Layer Gravity Settler," *Trans. Inst. Chem. Engrs.*, **53**, 61 (1975).

Beggs, H. D., and J. P. Brill, "An Experimental Study of Two-Phase Flow in Inclined Pipes," Prepr. 4007, *Proc. 47th Ann. Fall Meet. Soc. Pet. Eng. AIME, San Antonio* (Oct., 1972).

Bendiksen, K. H., "An Experimental Investigation of the Motion of Long Bubbles in Inclined Tubes," *Int. J. Multiph. Flow*, **10**, 467 (1984).

Bonnecaze, R. H., W. Erskine, and E. J. Greskovich, "Hold-up and Pressure Drop for Two-Phase Slug Flow in Inclined Pipelines," *Am. Inst. Chem. Eng. J.*, **17**, 1109 (1971).

Charles, M. E., and L. U. Lilleleht, "Correlation of Pressure Gradients for the Stratified Laminar-Turbulent Pipe Flow of Two Immiscible Liquids," *Can. J. Chem. Eng.*, 47 (Feb., 1966).

Dukler, A. E., and M. G. Hubbard, "A Model for Gas-Liquid Flow in Horizontal and Near-Horizontal Tubes," *Ind. Eng. Chem. Fundam.*, **14**, 337 (1975).

Foussat, A. J. M., and J. P. Hulin, "Vertical Liquid-Liquid and Liquid-Gas Two-Phase Flow Measurements with a Vortex Flowmeter," *Proc. IUTAM Symp on Measuring Techniques in Gas-Liquid Two-phase Flow, July 5–8, 1983, Nancy (France)*, G. Cognet, J. M. Delhaye, eds., Springer, 651 (1984).

Jones, O. C., and J. M. Delhaye, "Transient and Statistical Measurement Techniques for Two-phase Flow (A Critical Review)," *Int. J. Multiph. Flow*, **3**, 89 (1976).

Kobori, T., and M. Terada, "Application of the Needle-type Void Meter to Blow-down Tests," *Proc. CSNI Specialist Meet. on Transient Two-phase Flow*, Paris 699 (1978).

Lighthill, J. *Waves in Fluids*, Cambridge, Ch. 4 (1978).

Maneri, C. C., and N. Zuber, "An Experimental Study of Plane Bubbles Rising at Inclination," *Int. J. Multiph. Flow*, **1**, 623 (1974).

Mattar, L., and G. A. Gregory, "Air-Oil Slug Flow in an Upward-Inclined Pipe. I: Slug Velocity, Hold-up, and Pressure Gradient," *J. Can. Petr. Technol.*, **13**, 69 (1974).

Nicolas, Y., and F. J. Witterholt, "Measurement of Multiphase Flow," *Proc. 47th Ann. Fall Meet. Soc. Pet. Eng. AIME, San Antonio* (Oct., 1972).

Reimann, J., A. John, and S. Muller, "Bestimmung der Stromungs in horizontaler Luft-Wasser sowie Dampf-Wasser Stromung mit einer localen Impedanz Sonde," Rept. KFK 2527, Karlsruhe Nuc. Res. Cen. (1977).

Russel, T. W. F., and M. E. Charles, "The Effect of the Less Viscous Liquid in the Laminar Flow of Two Immiscible Liquids," *Can. J. Chem. Eng.*, 18 (Feb., 1959).

Singh, G., and P. Griffith, "Determination of the Pressure Drop Optimum Pipe Size for a Two-phase Slug Flow in an Inclined Pipe," *J. Eng. Ind.*, **92**, 717 (1970).

Taitel, Y., and A. E. Dukler, "A Model for Predicting Flow Regime Transitions in Horizontal and Near-horizontal Flow," *AIChE J.*, **22**, 47 (1976).

Taitel, Y., D. Bornea, and A. E. Dukler, "Modeling Flow Pattern Transitions for Steady Upward Gas-Liquid Flows in Vertical Tubes," *AIChE J.*, **26**, 345 (1980).

Vince, M. A., and R. T. Lahey, "Flow Regime Identification and Volume Fraction Measurement Techniques in Two-phase Flows," Nuclear Regulatory Comm. Rept. NUREG/CR1692 (1980).

Zakin, J. L., L. Pinaire, and M. E. Borgmeyer, "Transport of Oils as Oil-in-Water Emulsions," *ASME Trans.*, **101**, 100 (1979).

Zukoski, E. E., "Influence of Viscosity, Surface Tension, and Inclination Angle on the Motion of Long Bubbles in Closed Tubes," *J. Fluid. Mech.*, **25**, 821 (1966).

Manuscript received Feb. 9, 1987, and revision received Dec. 29, 1987.